Science of the Total Environment 628–629 (2018) 1609–1616

Contents lists available at ScienceDirect

Science of the Total Environment

journal homepage: www.elsevier.com/locate/scitotenv

Developing and interpreting aqueous functional assays for comparative property-activity relationships of different nanoparticles

Justin M. Kidd [a], David Hanigan [d], Lisa Truong [b], Kiril Hristovski [c], Robert Tanguay [b], Paul Westerhoff [a,*]

[a] Nanosystems Engineering Research Center for Nanotechnology-Enabled Water Treatment, Arizona State University, School of Sustainable Engineering and the Built Environment, Tempe, AZ 85287-3005, United States
[b] Department of Environmental and Molecular Toxicology, Environmental Health Sciences Center, Marine and Freshwater Biomedical Sciences Center, Oregon State University, Corvallis, OR 97331-7301, United States
[c] The Polytechnic School, Fulton Schools of Engineering, Arizona State University, Mesa, AZ 85212, United States
[d] Department of Civil and Environmental Engineering, University of Nevada, Reno, Nevada 89557-0258, United States

HIGHLIGHTS

- A framework to compare ENM properties to their environmental behavior was proposed.
- There is a high reproducibility of functional assay results for all nanomaterials tested.
- Some functional assays may be surrogates for other assays, reducing experimental time and cost.
- Activity-profiling radar plots provide a unique way to visualize potential hazards of ENMs.

GRAPHICAL ABSTRACT

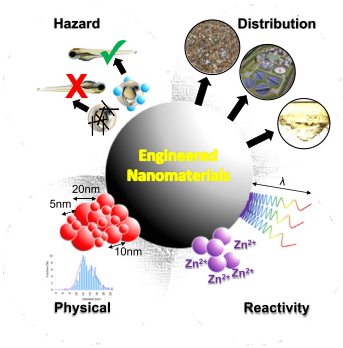

ARTICLE INFO

Article history:
Received 11 November 2017
Received in revised form 8 February 2018
Accepted 9 February 2018
Available online 28 February 2018

Editor: D. Barcelo

Keywords:
Nanoparticle
Water
Exposure
Hazard
Fate

ABSTRACT

It is difficult to relate intrinsic nanomaterial properties to their functional behavior in the environment. Unlike frameworks for dissolved organic chemicals, there are few frameworks comparing multiple and inter-related properties of engineered nanomaterials (ENMs) to their fate, exposure, and hazard in environmental systems. We developed and evaluated reproducibility and inter-correlation of 12 physical, chemical, and biological functional assays in water for eight different engineered nanomaterials (ENMs) and interpreted results using activity-profiling radar plots. The functional assays were highly reproducible when run in triplicate (average coefficient of variation [CV] = 6.6%). Radar plots showed that each nanomaterial exhibited unique activity profiles. Reactivity assays showed dissolution or aggregation potential for some ENMs. Surprisingly, multi-walled carbon nanotubes (MWCNTs) exhibited movement in a magnetic field. We found high inter-correlations between cloud point extraction (CPE) and distribution to sewage sludge ($R^2 = 0.99$), dissolution at pH 8 and pH 4.9 ($R^2 = 0.98$), and dissolution at pH 8 and zebrafish mortality at 24 hpf ($R^2 = 0.94$). Additionally, most ENMs tend to distribute out of water and into other phases (i.e., soil surfaces, surfactant micelles, and sewage sludge). The activity-profiling radar plots provide a framework and estimations of likely ENM disposition in the environment.

* Corresponding author.
E-mail address: p.westerhoff@asu.edu (P. Westerhoff).

https://doi.org/10.1016/j.scitotenv.2018.02.107
0048-9697/

1. Introduction

Relative to work with dissolved organic chemicals, there are few strategies to compare the multiple and inter-related properties of engineered nanomaterials (ENMs) to their fate, exposure, and hazard in environmental systems (Westerhoff & Nowack, 2013; Yokel & MacPhail, 2011). Frameworks exist that relate intrinsic properties (e.g. crystal lattice structure) to negative environmental impacts (e.g. redox potential, band gap, cellular dysfunction) (Naldoni et al., 2012; Zhang et al., 2012; George et al., 2011), but such mechanistic models have not yet been integrated into predictive mechanistic fate and transport models for ENMs in water or soils (Gottschalk et al., 2009; Darlington et al., 2009; Praetorius et al., 2012) or absorption, distribution, metabolism, and excretion (ADME) models for whole organism exposures (Selick et al., 2002; Yu & Adedoyin, 2003). High-throughput testing platforms for hazards or toxicity have been developed to assess ENM functional behavior in complex systems (Mandrell et al., 2012; Truong et al., 2013; Cassano et al., 2016; Goldberg et al., 2015; Winkler, 2016; Silva et al., 2014; Vazquez-Munoz et al., 2017). For example, zebrafish are used as a sensitive, relevant whole-animal system to define the inherent toxicity of ENMs, chemicals, and complex mixtures (Allan et al., 2012; Kim et al., 2013; Chen et al., 2013; Corvi et al., 2012; Kim et al., 2012; Liu et al., 2012; Lin et al., 2013). Other emerging testing platforms for ENMs include surface photocatalytic reactivity using a methylene blue dye redox system (Corredor et al., 2015; Khaksar et al., 2015; Sabry et al., 2016), hydrophobicity using an octanol-water partitioning system (Nel et al., 2009; Xiao & Wiesner, 2012; Hristovski et al., 2011), and magnetization using external magnets (Shahbazi-Gahrouei et al., 2013; Park et al., 2013). Assays for ENM attachment behavior in different aqueous solutions onto different substrates (e.g., suspended lipid bilayers) have also been developed (Liu & Chen, 2015; Pokhrel et al., 2013a; Pokhrel et al., 2013b). Nevertheless, we still lack frameworks or assays to assess and interpret how the unique properties that arise at the nanoscale (e.g., magnetisms, plasmonic resonance) impact ENM environmental fate and ecotoxicity. Furthermore, while many studies include a single or few assays on a specific ENM, current literature lacks studies including multiple assays on the same ENM.

At least two approaches exist for utilizing functional assays as a tool to assess the relationships between ENM properties and environmental outcomes. First, functional assays can obtain rate or aggregation parameters for mechanistic fate modelling. Hendren et al. (2015) applied separate functional assays for dissolution rates and aggregation rates and developed a protocol to collect data suitable to parameterize nanomaterial fate and transport models. Second, functional assays can compare the relative activity of pollutants across multiple quadrants of activity-profiling plots. Crittenden et al. (2014) applied this method to compare the relative safety and sustainability of different chemicals by graphing numerous factors on a radar plot. Prior work on organic chemicals estimates activity using fugacity-based parameters and experimental functional assays (e.g., octanol-water partitioning coefficients). In this paper, we evaluated the applicability of nano-specific functional assays to develop activity profiles (i.e. radar plots for several ENMs).

This study's goal was to evaluate the suitability and reproducibility of functional assays that cover a wide range of behaviors exhibited by various ENMs. Our objective was to develop relationships between an ENM's physico-chemical properties and functionality and use those relationships to predict their fate and transport in the environment, not to obtain parameters for fate and transport modelling. Eight ENMs that exhibit unique properties (plasmon resonance, magnetism, dissolved ion delivery, etc.) and are used in commercial products were selected for evaluation in this study. First, we designed functional assays to measure reactivity, distribution, physical and hazard behavioral outcomes of ENMs. Desirable features of the assays were that they took <24 h and utilized small masses of ENMs. Second, the assay reproducibility was evaluated. Third, the inter-correlated relationships were determined among different functional assay results. Finally, a strategy was developed to plot and interpret the assay outcomes.

2. Methods and materials

2.1. Nanoparticle selection and quantification

Eight commercially relevant ENMs were used in this study: (1) Citrate-coated silver, (2) polyvinyl pyrrolidone-coated magnetite Fe_3O_4, (3) tannic acid-capped gold, (4) fluorescein-capped SiO_2, (5) colloidal SiO_2, (6) ZnO, (7) CeO_2, and (8) dispersed MWCNTs. (See Table S1 and Fig. S1 for manufacturer information). For non-biological functional assays, ENMs were purchased and received already dispersed in solution at concentrations between 20 mg/L and 200 mg/L. For non-biological functional assays, the ENM stock solutions were dispersed in 1 mM $NaHCO_3$ buffer at pH 7.4 ± 0.2 at a concentration of 5 mg/L. For biological functional assays, the ENM stock solutions were dispersed at 6 different concentrations in ultrapure water, and then diluted as described below. Triplicate samples were prepared for each nanoparticle dispersion used in the functional assays. Metal-based nanoparticles were quantified using inductively coupled plasma mass spectroscopy (ICP-MS) after digestion in 2% nitric acid (Speed et al., 2015; Lee et al., 2014; Bi et al., 2014; Mitrano et al., 2013; Reed et al., 2012) and MWCNTs were quantified using programmed thermal analysis (PTA) or UV/Vis light scattering (Doudrick et al., 2012). Additional nanoparticle analysis details are provided in the supporting information (SI).

2.2. Functional assays

Table 1 places the functional assays into activity-profiling quadrants (hazard, physical, reactivity, and distribution) and summarizes the functional assay methods, analytical tools, and quantitative output parameters. Although not inclusive of all possible activity endpoints, the table provides several possible assays that can be used to evaluate, plot, and interpret nanomaterial activity in the environment. Detailed descriptions of the functional assays are provided in the SI and briefly outlined here.

Unless otherwise stated, functional assays were conducted in either 40 mL glass vials with Teflon™ septa screw caps or 50 mL polypropylene centrifuge vials to minimize ENM losses onto the vessels. Assays involving agitation were conducted in a 45-rpm rotator table. ENMs were separated from ionic forms using 30 kDa centrifugal ultrafilters (Millipore, Ultracel Regenerated Cellulose Membrane, >90% Recovery). Samples were prepared for analysis within 1 h of completing the assay to prevent adsorption to vials and analyzed within 24 h. Individual ENMs were analyzed in triplicate for each functional assay to determine assay reproducibility. For the toxicity characteristic leaching procedure (TCLP) functional assay, the solution was adjusted to pH 4.9 to reflect the acidic conditions of a landfill and was conducted following the U.S. Environmental Protection Agency (EPA) standard method(USEPA, 1992). The TCLP assay was conducted to assess dissolution potential of the nanoparticles in landfill leachate solutions, and is not indicative of a toxicity assay.

The zebrafish ecotoxicity assay was conducted using a separate methodology than the other assays (Details in SI). Tropical 5D wild-type adult zebrafish embryos were collected, and the chorion was enzymatically removed using pronase to increase bioavailability. To track exposures, six concentrations were tested for each ENM using one animal per well in a 96-well plate. Each condition used 32 replicates. The 96-well plates (with embryos) were agitated overnight at 230 rpm on an orbital shaker. To track mortality and morphology responses, the zebrafish embryos were statically exposed until 120 h post fertilization (hpf). At 24 hpf, four developmental toxicity endpoints were assessed in each embryo: mortality at 24 hpf (MO24), developmental progression (DP), spontaneous movement (SM), and notochord distortion (NC). At 120 hpf, 18 developmental endpoints were assessed. The zebrafish

Table 1
Functional assays and dimensions used for eight nanoparticles. Size and polydispersity can be considered for both reactivity and physical activity profiling quadrants.

Activity profiling quadrant	Functional assay	# of assays	Method description	Analytical tool	Functional assay outcome parameter	Assay outcome mechanism
Reactivity	Magnetism	1	Removal of ENM from solution using magnet	ICP-MS/PTA	% Removed from solution	Ferro-magnetism
	Resonance wavelength	1	Wavelength scan from 200 to 800 nm to find wavelength and absorbance of optimal peak	UV–Vis Spectroscopy	Wavelength (λ)	Resonance
	Dissolution (pH 8.0)	1	Dissolution potential of ENMs in a basic aqueous matrix	ICP-MS/PTA	% Dissolution	Dissolution
	TCLP dissolution (pH 4.9)	1	Dissolution potential of ENMs in an acidic aqueous matrix	ICP-MS/PTA	% Dissolution	
Distribution	Cloud point extraction	1	Removal of ENM from solution using surfactant	ICP-MS/PTA	% ENM extraction from media	Hetero-aggregation
	Hydrophobicity	1	Octanol-water partitioning test	ICP-MS/PTA	% Distribution	
	Wastewater sludge partitioning	1	Partitioning of ENM to biomass collected from a local wastewater treatment facility	ICP-MS/PTA	% Distribution	
	Partitioning to sediment	1	Partitioning of ENM to IHSS sandy loam soil	ICP-MS/PTA	% Distribution	
Physical	Size	1	Light scattering method using 1 cm^3 quartz cuvettes	Dynamic Light Scattering (DLS)	Mean hydrodynamic diameter (nm)	Homo-aggregation
	Polydispersity	1	Light scattering method using 1 cm^3 quartz cuvettes	Dynamic Light Scattering (DLS)	Polydispersity	
Hazard	Zebrafish phenotype	21	Behavioral impact of ENM on tropical 5D wild-type zebrafish embryos	Zebrafish acquisition and analysis program (ZAAP)	Zebrafish developmental outcomes (absent v. present)	Biological Development
	Zebrafish toxicity	1	Toxicity impact of ENM on tropical 5D wild-type zebrafish embryos	Zebrafish acquisition and analysis program (ZAAP)	% Mortality	Biological toxicity

acquisition and analysis program (ZAAP), a custom program designed to inventory, acquire, and manage zebrafish data, was used to collect developmental endpoints as either present or absent. For the zebrafish toxicity and behavioral biological assays, we assigned a "1" to values that were absent and a "2" to values that were present.

3. Results and discussion

3.1. Reproducibility of functional assays

Table 2 summarizes functional assay reproducibility for each ENM with the coefficient of variation (CV), calculated using the following equation:

$$CV = \frac{\sigma}{|\mu|} \quad (1)$$

where σ is the standard deviation and $|\mu|$ is the absolute value of the mean.

For the nanoparticles and functional assays evaluated, approximately one quarter of the data sets had CV >10%, and only about 5% of the data sets had CV >30% (Table 2), indicating that these functional assays are highly reproducible. The zebrafish assays are evaluated on absence/presence of biological behavior or toxicity. The nominal values collected for those assays are unable to be analyzed by CV. Although not considered here, previous studies have evaluated the reproducibility of ENM toxicity on Zebrafish systems (Liu et al., 2017; Busquet et al., 2014).

Table 2
Coefficients of variation (CV) for the non-biological functional assays with 8 ENMs. Data are presented as percentages. Black-highlighted CVs are >30%. Grey-highlighted CVs are >10% (and <30%). The zebrafish assay data was collected as presence/absence so a CV was not obtainable.

Functional assays	Ag	Au	CeO_2	Fe_3O_4	MWCNT	SiO_2 - C	SiO_2 - F	ZnO
Size	20	5.9	0.4	9.8	4.8	0.6	4.3	0.3
Polydispersity	16	41	6.2	18	14	2.6	6.8	4.3
Magnetism	2.9	1.0	7.0	5.3	7.5	3.1	3.3	0.5
Resonance wavelength	0.2	0.1	0.5	0.3	0.2	0.0	0.3	0.2
Dissolution (pH 8)	9.8	9.3	34	17	0.0	14	11	7.1
Dissolution (pH 4.9)	4.0	5.7	6.1	15	0.0	24	25	4.5
Cloud point extraction	1.3	13	3.9	1.5	15	4.3	1.7	0.6
Hydrophobicity	1.3	4.1	1.4	3.3	39.7	4.2	3.7	3.0
WW sludge partitioning	1.1	1.0	15.6	3.4	5.7	3.3	2.1	1.7
Distribution to sediment	1.8	0.8	12.5	3.6	5.5	3.8	2.0	1.8

3.2. ENM comparisons for functional assay groupings

The functional assays are grouped into four environmental outcome quadrants: reactivity, distribution, physical, and hazard. The reactivity quadrant has measured outcomes that indicate ENM interactions with light (optical resonance), magnetic fields, or undergo dissolution. The distribution quadrant has measured outcomes that indicate potential ENM preference for non-aqueous phases (e.g. solids, solvents, micelles, sludge). The physical quadrant has measured outcomes that indicate ENM properties related to the system (1 mM $NaHCO_3$ water). The hazard quadrant has measured outcomes that indicate potential ENM interactions and hazards to Zebrafish development and Zebrafish toxicity. Results from each quadrant highlight the activity outcomes we observed experimentally. Additional assay outcomes can be found in the SI.

3.2.1. Nanomaterial property-reactivity relationships

Fig. 1A compares the fraction of ENMs that dissolved for the eight different nanoparticles in two environmental matrices (1 mM $NaHCO_3$ buffer [pH 8.0] or TCLP landfill leachate [pH 4.9]). Triplicate experiments showed highly reproducible results (Average SD = ±1.5% dissolution). ZnO was the only nanoparticle from the group of eight exhibiting >50% dissolution. The remaining seven nanoparticles had <20% dissolution. Given that literature(Telgmann et al., 2016; Liu & Hurt, 2010) show nano-Ag dissolution increases in low pH conditions, it was surprising that <20% of the silver dissolved in the functional assays under neutral or acidic pH. While the TCLP solution has a pH of 4.9, it also contains high acetate levels, which can influence the formation of $AgC_2H_3O_2$ particulates ($Ksp = 2.0 \times 10^{-3}$). Consequently, a lower amount of silver dissolution relative to the larger amount of zinc dissolution is reasonable.

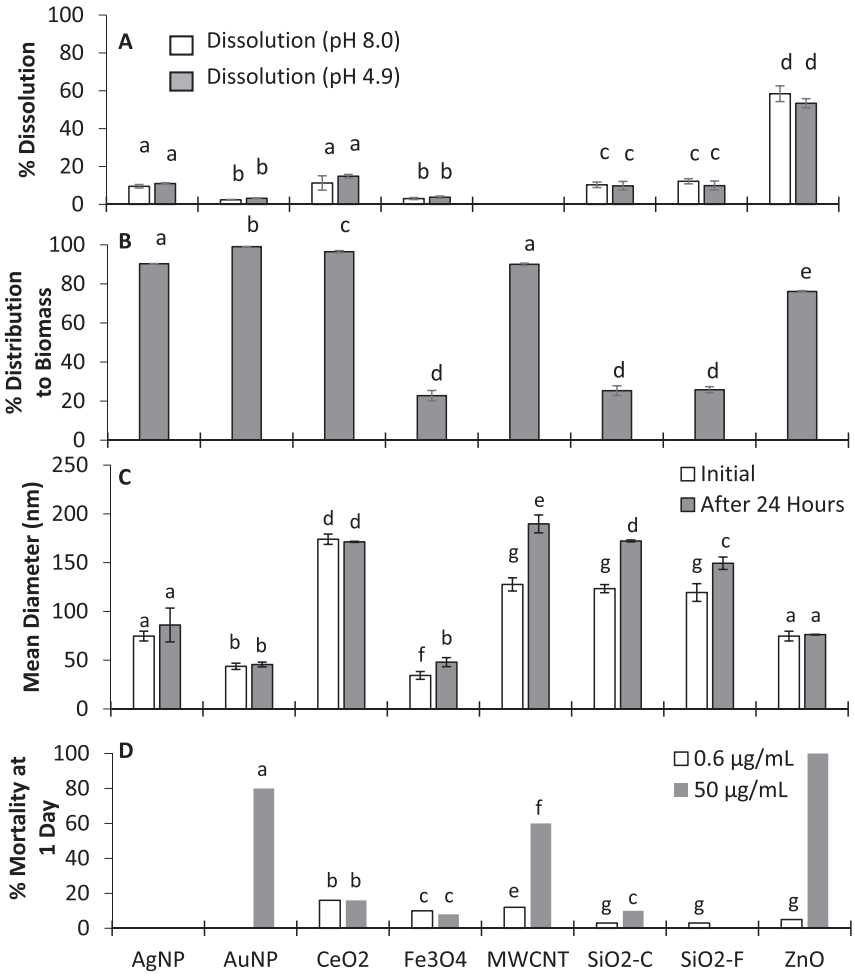

Fig. 1. Results for functional assays within each activity-profiling quadrant. A) % Dissolution of the 8 ENMs within the reactivity-activity quadrant. B) % Sorption to WW Biomass of the 8 ENMs within the distribution-activity quadrant. C) Mean diameters of the 8 ENMs within the physical-activity quadrant. D) % Mortality Values for the 8 ENMs within the hazard-activity quadrant (Other functional assay outcomes available in SI). Error bars represent 1 standard deviation based upon triplicate assays. Letters above bars denote statistically significant results at a 95% confidence level (ANOVA).

3.2.2. Nanomaterial property-distribution relationships

Fig. 1B compares hetero-aggregation potential for the eight ENMs by quantifying their distribution to wastewater biomass in 1 mM $NaHCO_3$ buffer (pH 8.0). Over 90% of Ag, Au, CeO_2, and MWCNT ENMs associated with biomass. In contrast, <30% of the mass of Fe_3O_4, SiO_2-colloidal, and SiO_2-Fluorescein associated with biomass. This information is useful when we begin exploring potential ENM environmental implications. ENMs with high distribution to sludge will likely be removed within wastewater treatment plants (WWTP). ENMs with a low distribution to sludge have a higher likelihood of passing through a WWTP and ending up in downstream waters.

3.2.3. Nanomaterial property-physical relationships

Fig. 1C shows the change in ENM size due to homo-aggregation before and after mixing in 1 mM $NaHCO_3$ buffer aqueous matrix for 24 h. MWCNTs, SiO_2-F and SiO_2-C had significantly increased changes in size during mixing. After 24 h of mixing, mean hydrodynamic diameters of Au, Ag, CeO_2, and ZnO ENMs remained similar to their initial dynamic light scattering (DLS) diameters, while SiO_2-colloidal, SiO_2-Fluorescein, MWCNTs, and Fe_3O_4 ENMs all showed significantly greater mean diameters. The high-aspect ratio of MWCNTs and their change in displacement during the assay could interfere with the DLS measurements, resulting in their variability in particle size, rather than homo-aggregation. After 24 h of mixing, polydispersity (Fig. S2) was below 0.35 for all ENMs, indicating that any homo-aggregation of ENMs during the assay allowed the ENMs to retain a relatively uniform size.

3.2.3.1. Nanomaterial property-hazard relationships. After 24 and 120 h of non-chorion embryonic exposure to each ENM, mortality from toxic effects was determined by counting number of dead zebrafish embryos after exposure. Mortality at applied ENM doses of 0.6 and 50 mg/L are shown in Fig. 1D. Percent mortality for all 8 ENMs at different dosing concentrations is shown in the SI. Au nanoparticles induced significant mortality at 30 mg/L or higher (38–81%), while MWCNTs showed induced mortality (60%) at 50 mg/L. ZnO was the most toxic because it induced significant mortality (>87%) at 10 mg/L or higher. The other five nanoparticles caused insignificant or low mortality (<15%) to the zebrafish.

In addition to using mortality, we also evaluated presence/absence of morphological and biological traits as a measure of ENM toxicity and indicator of zebrafish survival in the environment. A set of 21 of the 32 functional assays used here can also assess zebrafish phenotype and morphological traits upon ENM exposure. Here we only highlight endpoints that are statistically relevant for living embryos. Ag nanoparticles, while not eliciting a high percent mortality value, had an impact on zebrafish phenotype and morphology. At 5 mg/L Ag, 25% of the zebrafish exhibited developmental progress delays at 24 hpf and 25% exhibited excessive fluid accumulation around their yolk sac after 120 hpf. Exposure to CeO_2 at 50 mg/L resulted in 34% of zebrafish

exhibiting developmental progress delays at 24 hpf. Exposure to ZnO at 3.3 mg/L, which is slightly lower than the toxicity threshold for ZnO, resulted in 10% of the zebrafish having their brain absent or malformed. High mortality can mask the impact of ENMs on zebrafish phenotype and morphology because once a zebrafish embryo is dead, we no longer monitored its phenotype or morphological traits. In presence of ZnO at 24 hpf at a concentration of 10 mg/L, only 12.5% of the zebrafish population remained, and any phenotype or morphological responses observed of the zebrafish to the ZnO are insignificant when compared to the original population size. Additional information for the zebrafish mortality and phenotype assays is presented in the SI.

3.3. Inter-correlations of functional assays

Table 3 presents a correlation matrix for the functional assays and shows statistical parameters (P and R^2 values) based on linear relationships. No Zebrafish phenotype assays were shown because no correlations were found due to either (Westerhoff & Nowack, 2013) the significant mortality of Zebrafish, which prevents phenotypes from being observed, or (Yokel & MacPhail, 2011) no effect of ENMs on Zebrafish phenotype.

Four parameters showed high correlations with an $R^2 > 0.9$. Cloud point extraction (CPE) and wastewater sludge partitioning had an R^2 of 0.99. Both dissolution assays (pH 4.9 and 8.0) had an R^2 of 0.98. Zebrafish mortality (24 hpf) and the TCLP dissolution assay (pH 4.9) had an R^2 of 0.92. Zebrafish mortality (24 hpf) and the dissolution assay (pH 8.0) had an R^2 of 0.94. Plots of these four correlations are available in the SI.

These correlations lead to three basic inferences. First, most of the functional assays are independent from each other and thus represent different phenomena. Second, CPE appears to be a reasonable surrogate for measuring ENM partitioning to wastewater sludge. CPE chemistry is based on surfactants first attaching to the ENM, and then this newly functionalized surfactant-ENM becoming enmeshed within a surfactant miscelle that can be separated from liquid above its cloud point temperature (Duester et al., 2016). ENM attachment to and removal with wastewater biomass appears to involve interactions with biosurfactants and depends on ENM incorporation into physical structures (e.g., liposomes), and the heat treatment of biomass denatures such proteins and liposome structures (Kiser et al., 2012; Kiser et al., 2010). Thus, some similarity emerges in terms of ENM interaction with surfactants and enmeshment into physical structures (miscelles or cell wall biological structures) as a common mechanism in these two functional assays. It may be possible to use CPE to screen the potential for ENM removal at wastewater treatment plants, but more work to validate this hypothesis would be required where ENMs are added to a variety of sewage water matrices at different concentrations. Third, ENMs with higher dissolution potential correlate well in functional assays at pH 4.9 or 8.0 because both essentially are based on the potential of an ENM to undergo redox reactions that evolve to soluble ions. The presence of toxic metal ions in solution is recognized as source for adverse biological outcomes (Garner et al., 2015), but uncertainty exists about the mechanisms leading to adverse outcomes on zebrafish toxicity mechanisms for ENMs and their ionic counterparts (Bai et al., 2010; Shaw & Handy, 2011). However, it is reasonable that an adverse biological outcome (i.e., zebrafish mortality at 24 hpf) correlates with functional assays that indicate higher potential for release of soluble toxic metal ions. Overall, the correlation analysis is an important tool in understanding differences between ENMs and responses from the different functional assays and should not be misinterpreted as causal inference.

3.4. Developing activity-profiling radar plots

Activity-profiling radar plots (e.g., Fig. 2) show results of several ENM functional assays to give insight on nanoparticle behavior trends. For this work, we followed an approach used by Crittenden et al. (Crittenden et al., 2014) for developing chemical comparisons where the radar plot maps out all the functional assay responses to a specific chemical or, in this case, ENM.

There are different ways to normalize divisions on each spoke of the radar plot, but here the spokes on each dimension of the radar plots were given a ranking between 0 and 10, where each ranking number is associated with a corresponding range of outcomes. These outcome ranges typically fall under one of the following categories: (Westerhoff & Nowack, 2013) percent removals from different environmental phases (e.g., removal from water by magnet), (Yokel & MacPhail, 2011) percent distributions to different environmental phases (e.g., water to soil), (Naldoni et al., 2012) change in size (e.g., aggregation potential), and (Zhang et al., 2012) percent biological response (e.g., zebrafish percent

Table 3
Linear correlation matrix of the functional assays. Zebrafish phenotype assays were omitted because no correlation could be found. Results to the left of the correlation values of 1.00 are R^2 values. Zebrafish mortality (24 hpf) was analyzed for the ENM exposure concentration of 10 mg/L. Grey-shaded regions with bold numbers are functional assays with high correlations.

	Size	Polydispersity	Magnetism	Resonance Wavelength	Dissolution (pH 8.0)	TCLP Dissolution (pH 4.7)	Cloud Point Extraction	Hydrophobicity	WW Sludge Partitioning	Partitioning to Sediment	Zebrafish Mort @ 24 hpf
Size	1.00										
Polydispersity	0.02	1.00									
Magnetism	0.02	0.18	1.00								
Resonance Wavelength	0.37	0.05	0.01	1.00							
Dissolution (pH 8.0)	0.04	0.00	0.17	0.00	1.00						
TCLP Dissolution (pH 4.7)	0.04	0.00	0.18	0.00	**0.98**	1.00					
Cloud Point Extraction	0.00	0.12	0.05	0.13	0.00	0.01	1.00				
Hydrophobicity	0.23	0.12	0.15	0.06	0.08	0.10	0.11	1.00			
WW Sludge Partitioning	0.00	0.13	0.07	0.10	0.00	0.01	**0.99**	0.08	1.00		
Partitioning to Sediment	0.04	0.03	0.04	0.05	0.26	0.26	0.18	0.21	0.19	1.00	
Zebrafish Mort @ 24hpf	0.06	0.01	0.06	0.00	**0.94**	**0.92**	0.01	0.02	0.02	0.43	1.00

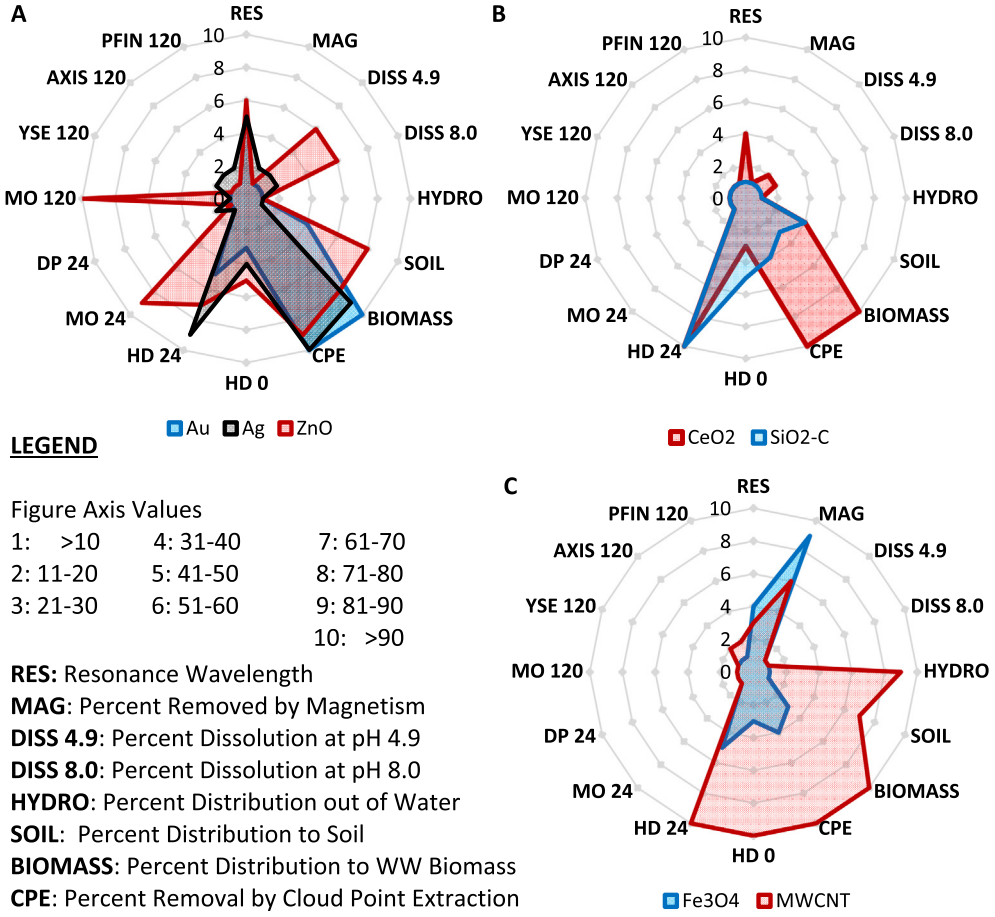

LEGEND

Figure Axis Values

1: >10	4: 31-40	7: 61-70
2: 11-20	5: 41-50	8: 71-80
3: 21-30	6: 51-60	9: 81-90
		10: >90

RES: Resonance Wavelength
MAG: Percent Removed by Magnetism
DISS 4.9: Percent Dissolution at pH 4.9
DISS 8.0: Percent Dissolution at pH 8.0
HYDRO: Percent Distribution out of Water
SOIL: Percent Distribution to Soil
BIOMASS: Percent Distribution to WW Biomass
CPE: Percent Removal by Cloud Point Extraction
HD 0: Hydrodynamic Diameter (nm) at T=0 Hrs
HD 24: Hydrodynamic Diameter (nm) at T=24 Hrs
MO 24: Percent Zfish Mortality at T=24 Hrs
DP 24: Percent Zfish Delayed Developmental Progression at T=24 Hrs
MO 120: Percent Zfish Mortality at T=120 Hrs
YSE 120: Percent Zfish With Excessive Fluid Accumulation around Yolk Sac at T=120 Hrs
AXIS 120: Percent Zfish With Abnormal Body Axis Curvature at T= 120 Hrs
PFIN 120: Percent Zfish With Abnormal or Missing Pectoral Fin.

Fig. 2. Activity Profile Radar Plots for the Comparison of Behavioral Trends of Different Engineered Nanomaterials. (A) Comparison of Au, Ag, and ZnO ENMs used as antimicrobials, (B) Comparison of CeO_2 and SiO_2-C ENMs used as chemical mechanical polishers, and (C) Comparison of Fe_3O_4 and MWCNT ENMs used as adsorbents for water treatment.

mortality). The radar plots are a unique tool to allow for the audience to visualize the grouping of nanomaterial physico-chemical property parameters together. Large scores in these parameters signals higher potential environmental activity. Radar plots allow for a comparison of the environmental activity of these different nanomaterials. Radar plots can be used as reference systems for reporting ENM exposure data, and thus can be used in standard protocols to determine nanomaterial property parameters. This provides a backbone for the future standardization of nanomaterials.

3.5. Radar plot comparisons for different nanoparticles

Fig. 2 contains activity profile radar plots to compare the behavioral trends of different engineered nanomaterials used in three different industrial applications. Fig. 2A compares three ENMs (Au, Ag, and ZnO), all which are used for their antimicrobial properties. Au and Ag have almost identical behavioral profiles with similar activity profiles for size distribution, resonance wavelength, low dissolution potential, etc. The major differences between the two ENMs is that Au ENMs were found to distribute to biomass and soil to a greater extent than Ag ENMs, while Ag ENMs were found to impact Zebrafish behavior more significantly than Au ENMs. ZnO was also similar to Au and Ag ENMs; however, it was found to have high dissolution potential and had high Zebrafish mortality (>90%). This result agrees with the current thought that ions that dissolve from metallic ENMs are largely responsible for the ecotoxic properties of ENMs. Fig. 2B compares two ENMs (CeO_2 and SiO_2-C), both of which are used in the semiconductor industry for chemical mechanical polishing. Both ENMs show a tendency to aggregate after 24 h. CeO_2 shows an affinity to adsorb to miscelles or cell wall biological structures. Fig. 2C compares two of the ENMs (Fe_3O_4 and MWCNTs), both of which are used for chemical pollutant adsorption in water treatment. Both ENMs show potential for magnetic separation. The Fe_3O_4 is intrinsically magnetic, whereas iron residuals in MWCNTs appear to give them their magnetic properties. While no reported toxicity mechanisms are associated with magnetism, literature suggests some ferrobacteria can align cells in a magnetic field (Uebe & Schuler, 2016). Emerging water treatment practices are attempting to reduce the effects of hard water by passing it through a magnetic field,

as a non-chemical alternative to water softening. MWCNTs tend to distribute to non-aqueous phases, which is probably associated with their hydrophobicity, while Fe_3O_4 nanoparticles remain in aqueous solutions. Thus, Fe_3O_4 may have a higher tendency to remain in effluent streams out of a wastewater treatment facility than MWCNTs. These observations give insight into the activity of these nanoparticles so that researchers and manufacturers can make more informed decisions when manufacturing ENMs and ENM-enabled products for consumer use. Additional radar plot comparisons were made and are available in the SI.

4. Conclusions

The development ENM activity profiles across a suite of different assays in these four activity quadrants provides valuable insight into how the physicochemical properties associated with ENMs can influence their inherent hazard and potential exposure routes. Elucidating these relationships via ENM activity-profiling radar plots should allow us to predict the efficacy and unintended consequences of ENMs in desired applications and would represent a unique strategy to efficiently and effectively anticipate potential environmental impacts. Overall, we demonstrated the reproducibility of functional assays for ENMs suspended in a standard 1 mM $NaHCO_3$ buffer, and we developed a strategy to plot and interpret the outcomes of the functional assays by using activity-profiling radar plots. Conducting functional assays and preparing activity-profiling radar plots for ENMs used in common products is an emerging way of visualizing potential environmental activity and impacts of ENMs, and these experiments allowed us to compare a multifunctional array of nanomaterial attributes to assess factors that may be important for both nanomaterial benefits and risks. Few correlations emerged between assays for a single ENM or among different ENM, potentially it difficult to group or read-across difficult among ENM classes.

Future work in this area would be to expand upon these functional assays and create new assays for different situations, including biological systems, chemical systems, and physical systems. It is also important for future work to streamline functional assays and make them higher throughput, allowing for a more rapid diagnosis of ENM material properties. If multiple assays continue to provide results similar to each other (e.g. CPE and distribution to WW Biomass), it may be feasible to use a specific functional assay as a surrogate for additional ones, which would reduce experimental time and costs. It would be of interest to harmonize a single test solution matrix (pH buffering capacity, ionic strength and composition, NP mass concentration ranges) across all assays, and such efforts could improve the ability to cross-correlate causal factors in observed trends (e.g., correlation between biomass sorption and zebrafish toxicity). Additionally, it would be beneficial to understand the dynamics between surface coatings and environmental composition on ENM behavior. Prior studies have shown that the coating of nanoparticles with surfactants (i.e. sodium dodecyl sulfate, SDS) increases ENM stability in solution (Gimbert et al., 2007) and mobility in porous media (Lecoanet et al., 2004). Environmental composition has also been shown to play a role in ENM behavior. Organic acids (i.e. humic and fulvic acids) have shown to inhibit aggregation of CNTs (Hyung et al., 2007), while proteins in biological fluids stabilize metallic ENMs regardless of their chemical composition, surface structure, and surface charge (Jurasin et al., 2016).

Acknowledgements

This research was partially funded by the U.S. Environmental Protection Agency (RD 83558001) and the National Science Foundation through the Nanosystems Engineering Research Center for Nano-Enabled Water Treatment (EEC 1449500).

Appendix A. Supplementary data

Supplementary data to this article can be found online at https://doi.org/10.1016/j.scitotenv.2018.02.107.

References

Allan, S.E., Smith, B.W., Tanguay, R.L., Anderson, K.A., 2012. Bridging environmental mixtures and toxic effects. Environ. Toxicol. Chem. 31 (12), 2877–2887.
Bai, W., Zhang, Z., Tian, W., et al., 2010. Toxicity of zinc oxide nanoparticles to zebrafish embryo: a physicochemical study of toxicity mechanism. J. Nanopart. Res. 12, 1645–1652.
Bi, X.Y., et al., 2014. Quantitative resolution of nanoparticle sizes using single particle inductively coupled plasma mass spectrometry with the K-means clustering algorithm. J. Anal. At. Spectrom. 29 (9), 1630–1639.
Busquet, F., Strecker, R., Rawlings, J., Belanger, S., Braunbeck, T., Carr, G., ... Halder, M., 2014. OECD validation study to assess intra- and inter-laboratory reproducibility of the zebrafish embryo toxicity test for acute aquatic toxicity testing. Regul. Toxicol. Pharmacol. 69 (3), 496–511.
Cassano, A., Robinson, M., Palczewska, A., Puzyn, T., Gajewicz, A., Tran, L., Manganelli, S., Cronin, M., 2016. Comparing the CORAL and Random Forest approaches for modelling the in vitro cytotoxicity of silica nanomaterials. Altern. Lab. Anim: ATLA 44 (6), 533.
Chen, J.F., Das, S.R., La Du, J., Corvi, M.M., Bai, C.L., Chen, Y.H., Liu, X.J., Zhu, G.N., Tanguay, R.L., Dong, Q.X., Huang, C.J., 2013. Chronic PFOS exposures induce life stage-specific behavioral deficits in adult zebrafish and produce malformation and behavioral deficits in F1 offspring. Environ. Toxicol. Chem. 32 (1), 201–206.
Corredor, C., Borysiak, M.D., Wolfer, J., Westerhoff, P., Posner, J.D., 2015. Colorimetric detection of catalytic reactivity of nanoparticles in complex matrices. Environ. Sci. Technol. 49 (6), 3611–3618.
Corvi, M.M., Stanley, K.A., Peterson, T.S., Kent, M.L., Feist, S.W., La Du, J.K., Volz, D.C., Hosmer, A.J., Tanguay, R.L., 2012. Investigating the impact of chronic atrazine exposure on sexual development in zebrafish. Birth Defects Res. B Dev. Reprod. Toxicol. 95 (4), 276–288.
Crittenden, J., Smetana, S., Pandit, A., 2014. Target Plots for Environmentally Responsible Selection of Chemicals. Center for Sustainable Engineering Electronic Library for Educational Modules.
Darlington, T.K., Neigh, A.M., Spencer, M.T., Guyen, O.T., Oldenburg, S.J., 2009. Nanoparticle characteristics affecting environmental fate and transport through soil. Environ. Toxicol. Chem. 28 (6), 1191–1199.
Doudrick, K., Herckes, P., Westerhoff, P., 2012. Detection of carbon nanotubes in environmental matrices using programmed thermal analysis. Environ. Sci. Technol. 46, 12246–12253.
Duester, L., Fabricius, A., Jakobtorweihen, S., Philippe, A., Weigl, F., Wimmer, A., Schuster, M., Nazar, M., 2016. Can cloud point-based enrichment, preservation, and detection methods help to bridge gaps in aquatic nanometrology? Anal. Bioanal. Chem. 408, 7551–7557.
Garner, K., Suh, S., Lenihan, H., Keller, A., 2015. Species sensitivity distributions for engineered nanomaterials. Environ. Sci. Technol. 49, 5753–5759.
George, S., Pokhrel, S., Ji, Z., Henderson, B.L., Xia, T., Li, L., Mädler, L., 2011. Role of Fe doping in tuning the band gap of TiO_2 for the photo-oxidation-induced cytotoxicity paradigm. J. Am. Chem. Soc. 133 (29), 11270–11278.
Gimbert, L., Hamon, R., Casey, P., Worsfold, P., 2007. Partitioning and stability of engineered ZnO nanoparticles in soil suspensions using flow field-flow fractionation. Environ. Chem. 4, 8–10.
Goldberg, E., Scheringer, M., Bucheli, T., Hungerbuhler, K., 2015. Prediction of nanoparticle transport behavior from physicochemical properties: machine learning provides insights to guide the next generation of transport models. Environ. Sci.: Nano 2 (4), 352–360.
Gottschalk, F., Sonderer, T., Scholz, R.W., Nowack, B., 2009. Modeled environmental concentrations of engineered nanomaterials (TiO_2, ZnO, Ag, CNT, fullerenes) for different regions. Environ. Sci. Technol. 43 (24), 9216–9222.
Hendren, C., Lowry, G., Unrine, J., Wiesner, M., 2015. A functional assay-based strategy for nanomaterial risk forecasting. Sci. Total Environ. 536, 1029–1037.
Hristovski, K., Westerhoff, P., Posner, J., 2011. Octanol-water distribution of engineered nanomaterials. J. Environ. Sci. Health, Part A: Toxic/Hazard. Subst. Environ. Eng. 46 (6), 636–647.
Hyung, H., Fortner, J., Hughes, J., Kim, J., 2007. Natural organic matter stabilizes carbon nanotubes in the aqueous phase. Environ. Sci. Technol. 41, 179–184.
Jurasin, D., Curlin, M., Capjak, I., Crnkovic, T., Lovric, M., Babic, M., Horak, D., Vrcek, I., Gajovic, S., 2016. Surface coating affects behavior of metallic nanoparticles in a biological environment. Beilstein J. Nanotechnol. 7, 246–262.
Khaksar, M., Boghaei, D.M., Amini, M., 2015. Synthesis, structural characterization and reactivity of manganese tungstate nanoparticles in the oxidative degradation of methylene blue. Comptes Rendus Chimie 18 (2), 199–203.
Kim, K.T., Jang, M.H., Kim, J.Y., Xing, B.S., Tanguay, R.L., Lee, B.G., Kim, S.D., 2012. Embryonic toxicity changes of organic nanomaterials in the presence of natural organic matter. Sci. Total Environ. 426, 423–429.
Kim, K., Truong, L., Wehmas, L., Tanguay, R.L., 2013. Silver nanoparticle toxicity in the embryonic zebrafish is governed by particle dispersion and ionic environment. Nanotechnology 24 (11), 115101.
Kiser, M., Ryu, H., Jang, H., Hristovski, K., Westerhoff, P., 2010. Biosorption of nanoparticles to heterotrophic wastewater biomass. Water Res. 44 (14), 4105–4114.
Kiser, M., Ladner, D., Hristovski, K., Westerhoff, P., 2012. Nanomaterial transformation and association with fresh and freeze-dried wastewater activated sludge: implications for testing protocol and environmental fate. Environ. Sci. Technol. 46 (13), 7046–7053.
Lecoanet, H., Bottero, J., Wiesner, M., 2004. Laboratory assessment of the mobility of nanomaterials in porous media. Environ. Sci. Technol. 38, 5164–5169.
Lee, S., et al., 2014. Nanoparticle size detection limits by single particle ICP-MS for 40 elements. Environ. Sci. Technol. 48 (17), 10291–10300.

Lin, S., Zhao, Y., Nel, A.E., Lin, S., 2013. Zebrafish: an *in vivo* model for nano EHS studies. Small (Weinheim an Der Bergstrasse, Germany) 9 (0), 1608–1618.
Liu, X., Chen, K.L., 2015. Interactions of graphene oxide with model cell membranes: probing nanoparticle attachment and lipid bilayer disruption. Langmuir 31 (44), 12076–12086.
Liu, J., Hurt, R., 2010. Ion release kinetics and particle persistence in aqueous nano-silver kinetics. Environ. Sci. Technol. 44 (6), 2169–2175.
Liu, R., Lin, S.J., Rallo, R., Zhao, Y., Damoiseaux, R., Xia, T., Lin, S., Nel, A., Cohen, Y., 2012. Automated phenotype recognition for zebrafish embryo based in vivo high throughput toxicity screening of engineered Nano-materials. PLoS One 7 (4).
Liu, R., Lin, S., Rallo, R., Zhao, Y., Damoiseaux, R., Xia, T., Shuo, L., Nel, A., Cohen, Y., 2017. Automated phenotype recognition for zebrafish embryo based in vivo high throughput toxicity screening of engineered nano-materials. PLoS One 7 (4), E35014.
Mandrell, D., Truong, L., Jephson, C., Sarker, M.R., Moore, A., Lang, C., Simonich, M.T., Tanguay, R.L., 2012. Automated zebrafish chorion removal and single embryo placement: optimizing throughput of zebrafish developmental toxicity screens. Jala 17 (1), 66–74.
Mitrano, D.M., et al., 2013. Silver nanoparticle characterization using single particle ICP-MS (SP-ICP-MS) and asymmetrical flow field flow fractionation ICP-MS (AF4-ICP-MS) (vol. 27, p. 1131, 2012). J. Anal. At. Spectrom. 28 (12), 1949.
Naldoni, A., Allieta, M., Santangelo, S., Marelli, M., Fabbri, F., Cappelli, S., Dal Santo, V., 2012. Effect of nature and location of defects on bandgap narrowing in black TiO_2 nanoparticles. J. Am. Chem. Soc. 134 (18), 7600–7603.
Nel, A., Madler, L., Velegol, D., Xia, T., Hoek, E., Somasundaran, P., Klaessig, F., Castranova, V., Thompson, M., 2009. Understanding biophysicochemical interactions at the nano-bio interface. Nat. Mater. 8, 543–557.
Park, H., Hwang, M., Lee, K., 2013. Immunomagnetic nanoparticle-based assays for detection of biomarkers. Int. J. Nanomedicine 8, 4543–4552.
Pokhrel, L., Dubey, B., Scheuerman, P., 2013a. Natural water chemistry (dissolved organic carbon, pH, and hardness) modulates colloidal stability, dissolution, and antimicrobial activity of citrate functionalized silver nanoparticles. Environ. Sci.: Nano 1, 45–54.
Pokhrel, L., Dubey, B., Scheuerman, P., 2013b. Impacts of select organic ligands on the colloidal stability, dissolution dynamics, and toxicity of silver nanoparticles. Environ. Sci. Technol. 47 (22), 12877–12885.
Praetorius, A., Scheringer, M., Hungerbühler, K., 2012. Development of environmental fate models for engineered nanoparticles: a case study of TiO_2 nanoparticles in the Rhine River. Environ. Sci. Technol. 46 (12), 6705–6713.
Reed, R.B., Ladner, D.A., Higgins, C.P., Westerhoff, P., Ranville, J.F., 2012. Solubility of nano-zinc oxide in environmentally and biologically important matrices. Environ. Toxicol. Chem. 31 (1), 93–99.
Sabry, R.S., Al-Haidarie, Y.K., Kudhier, M.A., 2016. Synthesis and photocatalytic activity of TiO_2 nanoparticles prepared by sol–gel method. J. Sol-Gel Sci. Technol. 78 (2), 299–306.
Selick, Harold E., Beresford, Alan P., Tarbit, Michael H., 2002. The emerging importance of predictive ADME simulation in drug discovery. Drug Discov. Today 7 (2), 109–116.
Shahbazi-Gahrouei, D., Abdolahi, M., Zarkesh-Esfahani, S., Laurent, S., Sermeus, C., Gruettner, C., 2013. Functionalized nanoparticles for the detection and quantitative analysis of cell surface antigen. Volume 2013. BioMed Research International.
Shaw, B., Handy, R., 2011. Physiological effects of nanoparticles on fish: a comparison of nanometals versus metal ions. Environ. Int. 37 (6), 1083–1097.
Silva, T., Pokhrel, L., Dubey, B., Tolaymat, T., Maier, K., Liu, X., 2014. Particle size, surface charge, and concentration dependent ecotoxicity of three organo-coated silver nanoparticles: comparison between general linear model-predicted and observed toxicity. Sci. Total Environ. 468-469, 968–976.
Speed, D., et al., 2015. Physical, chemical, and in vitro toxicological characterization of nanoparticles in chemical mechanical planarization suspensions used in the semiconductor industry: towards environmental health and safety assessments. Environ. Sci.: Nano 2 (3), 227–244.
Telgmann, L., Nguyen, M., Shen, L., Yargeau, V., Hintelmann, H., Metcalfe, C., 2016. Single particle ICP-MS as a tool for determining the stability of silver nanoparticles in aquatic matrixes under various environmental conditions, including treatment by ozonation. Anal. Bioanal. Chem. 408 (19), 5169–5177.
Truong, L., Tilton, S.C., Zaikova, T., Richman, E., Waters, K.M., Hutchison, J.E., Tanguay, R.L., 2013. Surface functionalities of gold nanoparticles impact embryonic gene expression responses. Nanotoxicology 7 (2), 192–201.
Uebe, R., Schuler, D., 2016. Magnetosome biogenesis in magnetotactic bacteria. Nat. Rev. Microbiol. 14 (10), 621–637.
USEPA, 1992. Method 1311 toxicity characteristic leaching procedure. SW-846 Test Methods for Evaluating Solid Waste, Physical/Chemical Methods. USEPA, Washington, D.C., pp. 1–35.
Vazquez-Munoz, R., Borrego, B., Juarez-Moreno, K., Garcia-Garcia, M., Mota Morales, J., Bogdanchikova, N., Huerta-Saquero, A., 2017. Toxicity of silver nanoparticles in biological systems: does the complexity of biological systems matter? Toxicol. Lett. 276, 11–20.
Westerhoff, P., Nowack, B., 2013. Searching for global descriptors of engineered nanomaterial fate and transport in the environment. Acc. Chem. Res. 46 (3), 844–853.
Winkler, David, 2016. Recent advances, and unresolved issues, in the application of computational modelling to the prediction of the biological effects of nanomaterials. Toxicol. Appl. Pharmacol. 299, 96–100.
Xiao, Y., Wiesner, M.R., 2012. Characterization of surface hydrophobicity of engineered nanoparticles. J. Hazard. Mater. 215–216.
Yokel, R.A., MacPhail, R.C., 2011. Engineered nanomaterials: exposures, hazards, and risk prevention. Journal of Occupational Medicine and Toxicology 6 (1), 7–30.
Yu, H., Adedoyin, A., 2003. ADME–Tox in drug discovery: integration of experimental and computational technologies. Drug Discov. Today 8 (18), 852–861.
Zhang, H., Ji, Z., Xia, T., Meng, H., Low-Kam, C., Liu, R., Nel, A.E., 2012. Use of metal oxide nanoparticle band gap to develop a predictive paradigm for oxidative stress and acute pulmonary inflammation. ACS Nano 6 (5), 4349–4368.